

## RESEARCH ARTICLE SUMMARY

## CORONAVIRUS

## Age groups that sustain resurging COVID-19 epidemics in the United States

Mélodie Monod\*, Alexandra Blenkinsop\*, Xiaoyue Xi\*, Daniel Hebert\*, Sivan Bershan\*, Simon Tietze\*, Marc Baguelin, Valerie C. Bradley, Yu Chen, Helen Coupland, Sarah Filippi, Jonathan Ish-Horowitz, Martin McManus, Thomas Mellan, Axel Gandy, Michael Hutchinson, H. Juliette T. Unwin, Sabine L. van Elsland, Michaela A. C. Vollmer, Sebastian Weber, Harrison Zhu, Anne Bezancon, Neil M. Ferguson, Swapnil Mishra, Seth Flaxman†, Samir Bhatt†, Oliver Ratmann\*†, on behalf of the Imperial College COVID-19 Response Team

**INTRODUCTION:** After initial declines, in mid-2020, a sustained resurgence in the transmission of novel coronavirus disease (COVID-19) occurred in the United States. Throughout the US epidemic, considerable heterogeneity existed among states, both in terms of overall mortality and infection, but also in the types and stringency of nonpharmaceutical interventions. Despite these stark differences among states, little is known about the relationship between interventions, contact patterns, and infections, or how this varies by age and demographics. A useful tool for studying these dynamics is individual, age-specific mobility data. In this study, we use detailed mobile-phone data from more than 10 million individuals and establish a mechanistic relationship between individual contact patterns and COVID-19 mortality data.

**RATIONALE:** As the pandemic progresses, disease control responses are becoming increasingly nuanced and targeted. Understanding fine-scale patterns of how individuals interact with each other is essential to mounting an efficient public health control program. For example, the choice of closing workplaces, closing schools, limiting hospitality sectors, or prioritizing vaccination to certain popu-

lation groups should be informed by the demographics currently driving and sustaining transmission. To develop the tools to answer such questions, we introduce a new framework that links mobility to mortality through age-specific contact patterns and then use this rich relationship to reconstruct accurate transmission dynamics (see figure panel A).

**RESULTS:** We find that as of 29 October 2020, adults aged 20 to 34 and 35 to 49 are the only age groups that have sustained SARS-CoV-2 transmission with reproduction numbers (transmission rates) consistently above one. The high reproduction numbers from adults are linked both to rebounding mobility over the summer and elevated transmission risks per venue visit among adults aged 20 to 49. Before school reopening, we estimate that 75 of 100 COVID-19 infections originated from adults aged 20 to 49, and the share of young adults aged 20 to 34 among COVID-19 infections was highly variable geographically. After school reopening, we reconstruct relatively modest shifts in the age-specific sources of resurgent COVID-19 toward younger individuals, with less than 5% of SARS-CoV-2 transmissions attributable to children aged

0 to 9 and less than 10% attributable to early adolescents and teenagers aged 10 to 19. Thus, adults aged 20 to 49 continue to be the only age groups that contribute disproportionately to COVID-19 spread relative to their size in the population (see figure panel B). However, because children and teenagers seed infections among adults who are more transmission efficient, we estimate that overall, school opening is indirectly associated with a 26% increase in SARS-CoV-2 transmission.

**CONCLUSION:** We show that considering transmission through the lens of contact patterns is fundamental to understanding which population groups are driving disease transmission. Over time, the share of age groups among reported deaths has been markedly constant, and the data provide no evidence that transmission shifted to younger age groups before school reopening, and no evidence that young adults aged 20 to 34 were the primary source of resurgent epidemics since the summer of 2020. Our key conclusion is that in locations where novel, highly transmissible SARS-CoV-2 lineages have not yet become established, additional interventions among adults aged 20 to 49, such as mass vaccination with transmission-blocking vaccines, could bring resurgent COVID-19 epidemics under control and avert deaths. ■

The list of authors and their affiliations is available in the full article online.

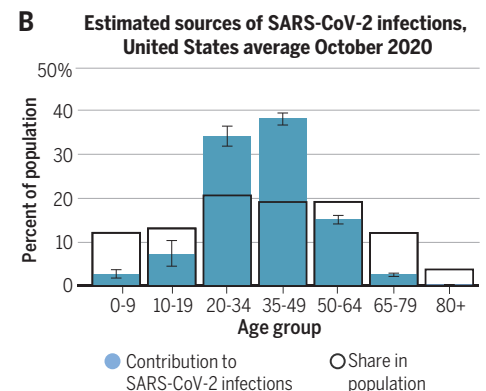
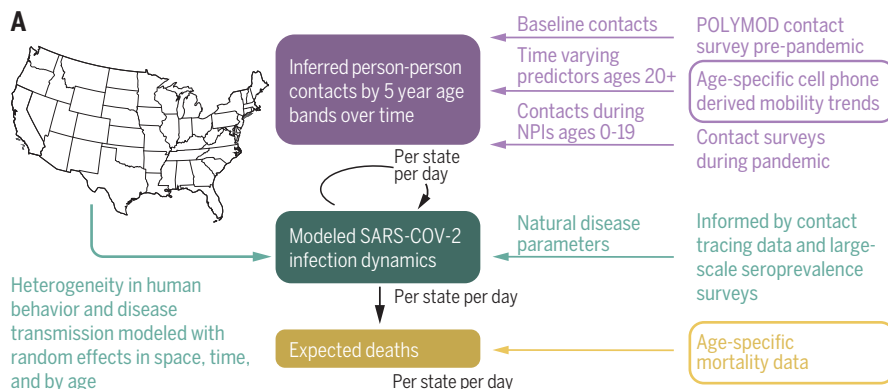
\*These authors contributed equally to this work.

†Corresponding author. Email: [oliver.ratmann@imperial.ac.uk](mailto:oliver.ratmann@imperial.ac.uk) (O.R.); [s.bhatt@imperial.ac.uk](mailto:s.bhatt@imperial.ac.uk) (S.B.); [s.flaxman@imperial.ac.uk](mailto:s.flaxman@imperial.ac.uk) (S.F.)

This is an open-access article distributed under the terms of the Creative Commons Attribution license (<https://creativecommons.org/licenses/by/4.0/>), which permits unrestricted use, distribution, and reproduction in any medium, provided the original work is properly cited.

Cite this article as M. Monod et al., *Science* 371, eabe8372 (2021). DOI: 10.1126/science.abe8372

**S READ THE FULL ARTICLE AT**  
<https://doi.org/10.1126/science.abe8372>



**Model developed to estimate the contribution of age groups to resurgent COVID-19 epidemics in the United States. (A)** Model overview. **(B)** Estimated contribution of age groups to SARS-CoV-2 transmission in October.

## RESEARCH ARTICLE

## CORONAVIRUS

## Age groups that sustain resurging COVID-19 epidemics in the United States

Mélie Monod<sup>1\*</sup>, Alexandra Blenkinsop<sup>1\*</sup>, Xiaoyue Xi<sup>1\*</sup>, Daniel Hebert<sup>2\*</sup>, Sivan Bershan<sup>3\*</sup>, Simon Tietze<sup>3\*</sup>, Marc Baguelin<sup>4</sup>, Valerie C. Bradley<sup>5</sup>, Yu Chen<sup>1</sup>, Helen Coupland<sup>4</sup>, Sarah Filippi<sup>1</sup>, Jonathan Ish-Horowicz<sup>1</sup>, Martin McManus<sup>1</sup>, Thomas Mellan<sup>4</sup>, Axel Gandy<sup>1</sup>, Michael Hutchinson<sup>5</sup>, H. Juliette T. Unwin<sup>4</sup>, Sabine L. van Elsland<sup>4</sup>, Michaela A. C. Vollmer<sup>4</sup>, Sebastian Weber<sup>6</sup>, Harrison Zhu<sup>1</sup>, Anne Bezancon<sup>3</sup>, Neil M. Ferguson<sup>4</sup>, Swapnil Mishra<sup>4</sup>, Seth Flaxman<sup>1†</sup>, Samir Bhatt<sup>4,7†</sup>, Oliver Ratmann<sup>1\*†</sup>, on behalf of the Imperial College COVID-19 Response Team

After initial declines, in mid-2020 a resurgence in transmission of novel coronavirus disease (COVID-19) occurred in the United States and Europe. As efforts to control COVID-19 disease are reintensified, understanding the age demographics driving transmission and how these affect the loosening of interventions is crucial. We analyze aggregated, age-specific mobility trends from more than 10 million individuals in the United States and link these mechanistically to age-specific COVID-19 mortality data. We estimate that as of October 2020, individuals aged 20 to 49 are the only age groups sustaining resurgent SARS-CoV-2 transmission with reproduction numbers well above one and that at least 65 of 100 COVID-19 infections originate from individuals aged 20 to 49 in the United States. Targeting interventions—including transmission-blocking vaccines—to adults aged 20 to 49 is an important consideration in halting resurgent epidemics and preventing COVID-19-attributable deaths.

Following worldwide spread of the novel severe acute respiratory syndrome coronavirus 2 (SARS-CoV-2), the implementation of large-scale nonpharmaceutical interventions has led to sustained declines in the number of reported SARS-CoV-2 infections and deaths from COVID-19 (1, 2). However, since mid-June 2020, the daily number of reported COVID-19 cases has been resurging in Europe and North America and in the United States (US) alone surpassed 40,000 daily reported cases on 26 June and 100,000 on 4 November 2020 (3). Demographic analyses have shown that the share of individuals aged 20 to 29 among reported cases increased most, suggesting that young adults may be driving resurging epidemics (4). However, reported COVID-19 case data may not be a reliable indicator of disease spread owing to the large proportion of asymptomatic COVID-19, increased testing, and changing testing behavior (5). Here, we use detailed, longitudinal, and age-specific population mobility and COVID-19 mortality data to estimate how nonpharma-

ceutical interventions, changing contact intensities, age, and other factors have interacted and led to resurgent disease spread. We test previous claims that resurgent COVID-19 is a result of increased spread from young adults, identify the population age groups driving SARS-CoV-2 spread across the US through 29 October 2020, and quantify changes in transmission dynamics since schools reopened.

Similar to many other respiratory diseases, the spread of SARS-CoV-2 occurs primarily through close human contact, which, at a population level, is highly structured (6). Prior to the implementation of COVID-19 interventions, contacts concentrated among individuals of similar age, were highest among school-aged children and teens, and were also common between children and teens and their parents and between middle-aged adults and the elderly (6). Since the beginning of the pandemic, these contact patterns have changed substantially (7–9). In the US, the Berkeley Interpersonal Contact Study indicates that in late March 2020, after stay-at-home orders were issued, the average number of daily contacts made by a single individual, also known as contact intensity, dropped to four or fewer contacts per day (9). Data from China show that infants and school-aged children and teens had almost no contact to similarly aged children and teens in the first weeks after stay-at-home orders and reduced contact intensities with older individuals (7). However, detailed human contact and mobility data have remained scarce, especially longitudinally, al-

though such data are essential to better understand the engines of COVID-19 transmission (10).

## Cell-phone data suggest similar rebounds in mobility across age groups

We compiled a national-level, aggregate mobility data set using cell phone data from >10 million individuals with Foursquare's location technology, Pilgrim (11), which leverages a wide variety of mobile device signals to pinpoint the time, duration, and location of user visits to locations such as shops, parks, or universities. Unlike the population-level mobility trends published by Google from cell phone geolocation data (12), the data are disaggregated by age. User venue visits were aggregated and projected to estimate, for each state, and two metropolitan areas, daily percentage changes in venue visits for individuals aged 18 to 24, 25 to 34, 35 to 44, 45 to 54, 55 to 64, and 65+ years relative to the baseline period 3 to 9 February 2020 (figs. S1 and S2 and supplementary materials).

Across the US as a whole, the mobility trends indicate substantial initial declines in venue visits, followed by a subsequent rebound for all age groups (Fig. 1A and fig. S1). During the initial phase of epidemic spread, trends declined most strongly among individuals aged 18 to 24 years across almost all states and metropolitan areas and subsequently tended to increase most strongly among individuals aged 18 to 24 in the majority of states and metropolitan areas (fig. S3), consistent with reopening policies for restaurants, night clubs, and other venues (10, 13, 14). Yet, considering both the initial decline and subsequent rebound until 28 October 2020, our data indicate that mobility levels among individuals aged <35 years have not increased above those observed among older individuals (Fig. 1B and fig. S3).

Mobile-phone signals are challenging to analyze, owing e.g., to daily fluctuations in the user panel providing location data, imprecise geolocation measurements, and changing user behavior (15). We cross-validated the inferred mobility trends against age-specific mobility data from a second mobile phone intelligence provider, Emodo. This second data set quantified the daily proportions of age-stratified users who spent time outside their home location and also showed no evidence for faster mobility rebounds among young adults aged <35 years as compared to older age groups (see supplementary materials). Although other age-specific behavioral differences in, for example, consistent social distancing, mask use, duration of visits, or types of venues visited could also explain age-specific differences in transmission risk (10, 13, 14, 16, 17), these observations nonetheless led us to hypothesize that the resurgent epidemics in the US

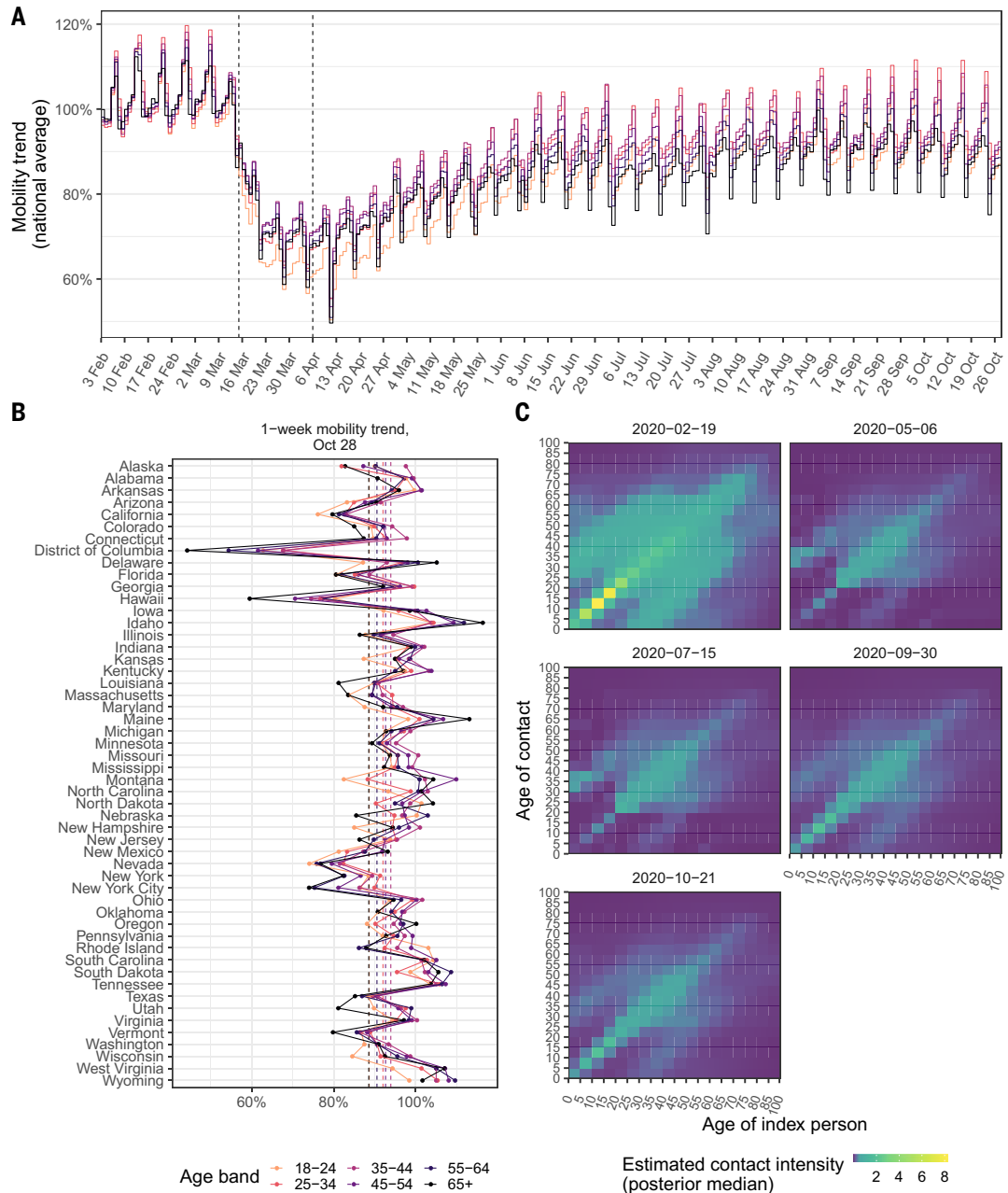
<sup>1</sup>Department of Mathematics, Imperial College London, London, UK. <sup>2</sup>Foursquare Inc., New York, NY, USA. <sup>3</sup>Emodo, San Francisco, CA, USA. <sup>4</sup>MRC Centre for Global Infectious Disease Analysis; and the Abdul Latif Jameel Institute for Disease and Emergency Analytics (J-IDEA), School of Public Health, Imperial College London, London, UK. <sup>5</sup>Department of Statistics, University of Oxford, Oxford, UK. <sup>6</sup>Novartis Pharma AG, Basel, Switzerland. <sup>7</sup>Section of Epidemiology, Department of Public Health, University of Copenhagen, Denmark.

\*These authors contributed equally to this work.

†Corresponding author. Email: oliver.ratmann@imperial.ac.uk (O.R.); s.bhatt@imperial.ac.uk (S.B.); s.flaxman@imperial.ac.uk (S.F.)

**Fig. 1. Mobility trends and estimated time evolution of contact intensities in the United States.**

(A) National, longitudinal mobility trends for individuals aged 18 to 24, 25 to 34, 35 to 44, 45 to 54, 55 to 64, and 65+, relative to the baseline period 3 February to 9 February 2020. Projected per capita visits standardized daily visit volumes by the population size in each location and age group. The vertical dashed lines show the dip and rebound dates since mobility trends began to decrease and increase, which were estimated from the time-series data. (B) One-week average of age-specific mobility trends between 22 October 2020 and 28 October 2020 across the United States. (C) Inferred time evolution of contact intensities in California, calculated with Eq. 4.



may not be driven by increased transmission from young adults aged 20 to 34.

**Reconstructing human contact patterns and SARS-CoV-2 transmission**

To test this hypothesis and disentangle the various factors, we incorporated the mobility data into a Bayesian contact-and-infection model that describes time-changing contact and transmission dynamics at state- and metropolitan area-level across the US. For the time period prior to changes in mobility trends, we used data from pre-COVID-19 contact surveys (6) and each location’s age composition and population density to predict contact intensities between individuals grouped in 5-year

age bands (figs. S4 to S6), similar to (18). On weekends, contact intensities between school-aged children and teens are lower than on weekdays, whereas intergenerational contact intensities are higher. In the model, the observed age-specific mobility trends of Fig. 1 are then used to estimate in each location (state or metropolitan area) daily changes in age-specific contact intensities for individuals aged 20 and above. For younger individuals, for whom mobility trends are not recorded, contact intensities during school closure periods were set to estimates from two contact surveys conducted after COVID-19 emergence (7, 8). After school reopening in August 2020, relative changes in disease-relevant contacts from

and to children and teens aged 0 to 19 were estimated through the model. Contact intensities between children and teens were modeled and estimated separately, to account for potentially lower or higher disease-relevant contacts between children and teens in the context of existing nonpharmaceutical interventions within and outside schools (see materials and methods). As in (19), the model further incorporates random effects in space, in time, and by age to allow for unobserved, potential age-specific factors that could modulate disease-relevant contact patterns. These random effects enabled us to identify signatures of age-specific, behavioral drivers of SARS-CoV-2 transmission beyond the mobility

Downloaded from https://www.science.org on March 22, 2024

data in Fig. 1 that may underlie the highly heterogeneous epidemic trajectories across the US. Finally, the reconstructed contact intensities are used in the model to estimate the rate of SARS-CoV-2 transmission, and subsequently infections and deaths. The summary figure provides a model overview, and full details are in the supplementary materials.

### Estimated disease dynamics closely reproduce age-specific COVID-19-attributable death counts

The contact-and-infection model was fitted to the Foursquare mobility trends and to age-specific, COVID-19-attributed mortality time-series data, which we recorded daily from publicly available sources in 42 US states, the District of Columbia, and New York City since 15 March 2020 (fig. S7 and supplementary materials). Our overall rationale was that, reflecting the highly structured nature of human contacts, transmissions from age groups are received by specific other age groups, and mortality accrues in the age groups receiving infections. Thus, working back from the time evolution of reliably documented, age-specific COVID-19-attributable deaths, it is possible to reconstruct age-specific drivers of transmission during particular time periods. Inference was performed in a Bayesian framework and restricted to 38 US states, the District of Columbia, and New York City with at least 300 COVID-19-attributed deaths, giving a total of 8676 observation days. The estimated disease dynamics closely reproduced the age-specific COVID-19 death counts (fig. S8).

Figure 2 illustrates the model fits for New York City, Florida, California, and Arizona, showing that the inferred epidemic dynamics differed markedly across locations. For example, in New York City, the epidemic accelerated for at least 4 weeks since the 10th cumulative death and until age-specific reproduction numbers started to decline, resulting in an epidemic of large magnitude, as shown through the estimated number of infectious individuals (Fig. 2, middle column). Subsequently, we find that reproduction numbers from all age groups were controlled to well below one, except for individuals aged 20 to 49 (Fig. 2, rightmost column), resulting in a steady decline of infectious individuals. In the model, children and teens returned to their pre-lockdown contact intensities on 24 August 2020 or later, depending on when state administrations no longer mandated statewide school closures, and relative decreases or increases in their disease-relevant contact intensities after school reopening were estimated. Concomitantly, reproduction numbers from children aged 0 to 9 and teens aged 10 to 19 increased, but as of the last observation week in October 2020, we find no strong evidence that their reproduction

numbers have exceeded one at the population level in most states and metropolitan areas considered. Detailed situation analyses for all locations are presented in the supplementary materials.

### SARS-CoV-2 transmission is sustained primarily from age groups 20 to 49

Figure 3 summarizes the epidemic situation for all states and metropolitan areas evaluated and the age groups that sustain COVID-19 spread. In the last observation week in October 2020, the estimated reproduction number across all locations evaluated was highest from individuals aged 35 to 49 [1.39 (1.34–1.44)] and 20 to 34 [1.29 (1.24–1.36)], and around one for age groups 10 to 19 and 50 to 64 (tables S1 and S2). These trends across age groups were largely consistent over time. The primary mechanisms underlying the high reproduction numbers from 20- to 49-year-olds are that at the population level, adults aged 20 to 49 naturally have most contacts with other adults aged 20 and above, who are more susceptible to COVID-19 than younger individuals, paired with increasing mobility trends for these age groups since April 2020 (Fig. 1 and fig. S6). In addition, from the death time-series data, the model inferred characteristic random effect signatures in time and by age across locations (fig. S9), which indicate elevated transmission risk per venue visit for individuals aged 20 to 49 relative to other age groups. Figure S10 visualizes the combined, estimated effects of mobility and behavior on transmission risk and reveals, together with Fig. 3, considerable heterogeneity in age-specific transmission dynamics across locations. Although the model consistently estimates effective reproduction numbers close to or above one across all locations from adults aged 35 to 49, disease dynamics are more variable from young adults aged 20 to 34, with some states (Arizona, Florida, Texas) showing sustained transmission from young adults in May and June, and other states (e.g., Colorado, Illinois, Wisconsin) showing sustained transmission from young adults since August. This suggests that additional interventions among adults aged 20 to 49, including rapid mass vaccination if vaccines prove to block transmission, could bring resurgent COVID-19 epidemics under control.

### The majority of COVID-19 infections originate from age groups 20 to 49

To quantify how age groups contribute to resurgent COVID-19, it is not enough to estimate reproduction numbers, because reproduction numbers estimate the number of secondary infections per infectious individual, and the number of infectious individuals varies by age as a result of age-specific susceptibility gradients and age-specific contact exposures.

We therefore considered the reconstructed transmission flows and calculated from the fitted model the contribution of each age group to new infections in each US location over time. Across all locations evaluated, we estimate that until mid-August 2020, before schools were considered to reopen in the first locations in the model, the percentage contribution to onward spread was 41.1% (40.7 to 41.4%) from individuals aged 35 to 49, compared with 2.1% (1.6 to 2.8%) from individuals aged 0 to 9, 4.0% (3.5 to 4.6%) from individuals aged 10 to 19, 34.7% (33.9 to 35.5%) from individuals aged 20 to 34, 15.3% (14.8 to 15.8%) from individuals aged 50 to 64, 2.5% (2.2 to 2.9%) from individuals aged 65 to 79, and 0.3% (0.3 to 0.3%) from individuals aged 80+ (table S4). Spatially, the contribution of adults aged 35 to 49 was estimated to be markedly homogeneous across states, whereas the estimated contributions of young adults aged 20 to 34 to COVID-19 spread tended to be higher in southern, southwestern, and western regions of the US (Fig. 4), in line with previous observations (4).

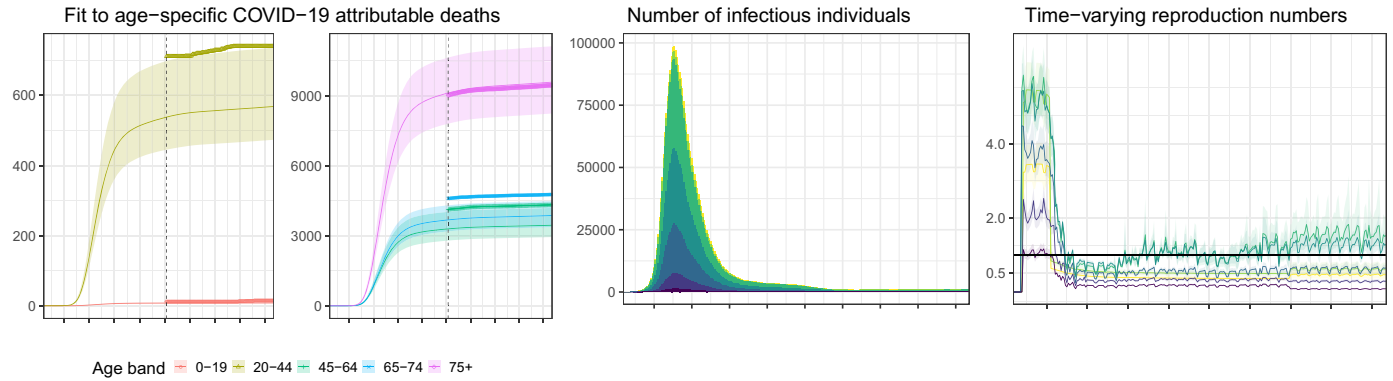
### No substantial shifts in age-specific disease dynamics over time

Over time, we found that the shares of age groups among the observed COVID-19-attributable deaths were markedly constant (Fig. 5A and fig. S11), which stands in contrast to the large fluctuations in the share of age groups among reported cases (4). To test for shifts in the share of age groups among COVID-19 infections, we next back-calculated the number of expected, age-specific infections per calendar month of aggregated COVID-19-attributable deaths using meta-analysis estimates of the age-specific COVID-19 infection fatality ratio (20). This empirical analysis suggested no statistically significant trends in the share of age groups among COVID-19 infections (Fig. 5B and fig. S12), which is further supported by model estimates (Fig. 5C and fig. S13). On the basis of the combined mobility and death data, we find that the reconstructed fluctuations in age-specific reproduction numbers had a relatively modest impact on the contribution of age groups to onward spread over time, and no evidence that young adults aged 20 to 34 were the primary source of resurgent COVID-19 in the US over the summer of 2020. These results underscore that, when testing rates are heterogeneous and not population representative, it is challenging to determine the age-specific pattern of transmission based only on reported case data.

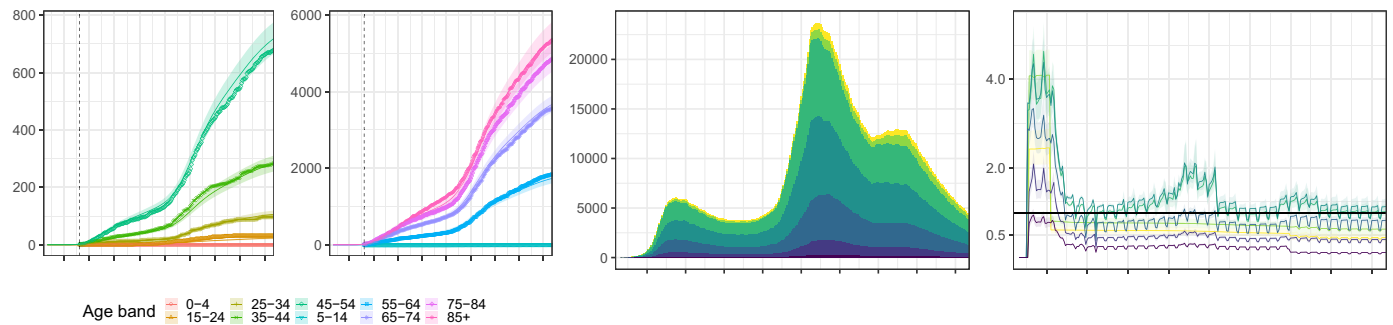
### School reopening has not resulted in substantial increases in COVID-19-attributable deaths

Between August and October 2020, school closure mandates have been lifted in 39 out of 40 of the US locations evaluated in this study

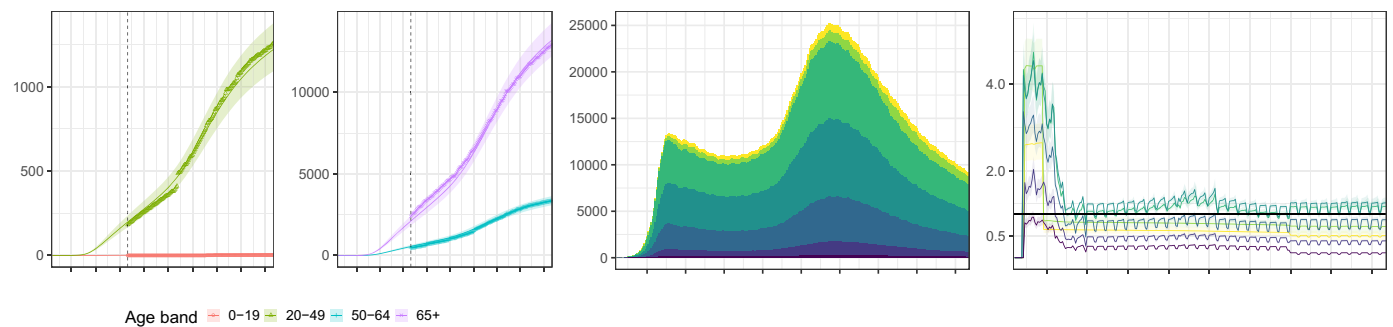
New York City



Florida



California



Arizona

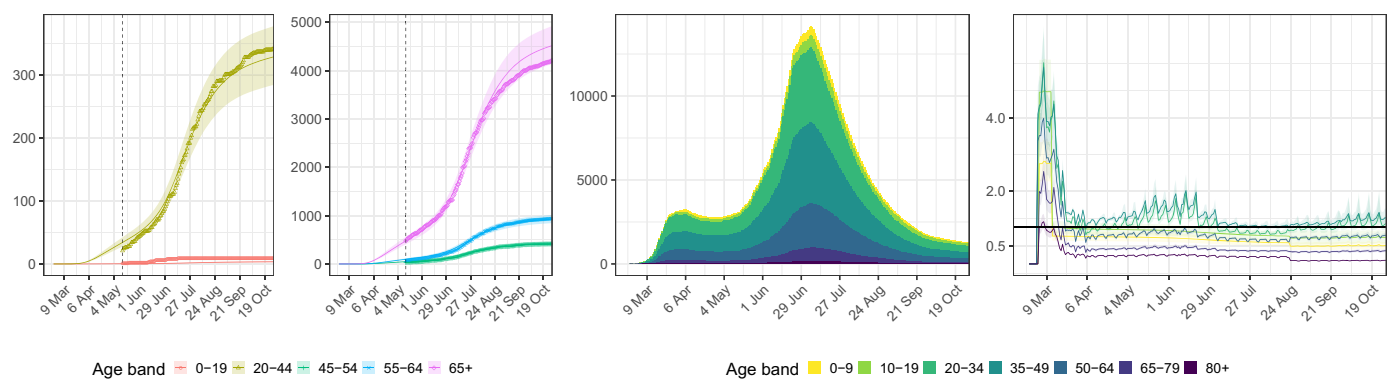
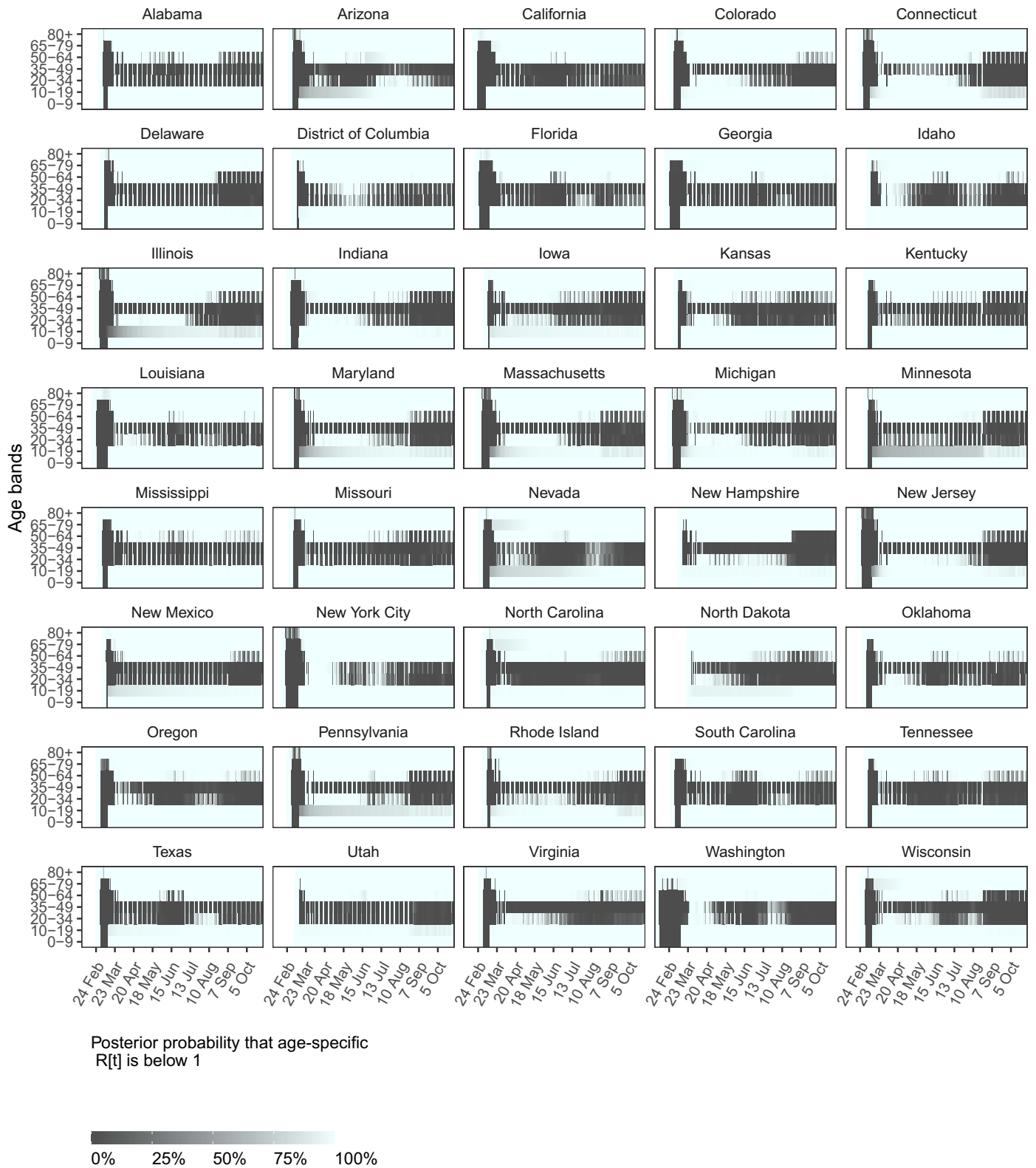


**Fig. 2. Model fits and key generated quantities for New York City, California, Florida, and Arizona.** (Left) Observed cumulative COVID-19 mortality data (dots) versus posterior median estimate (line) and 95% credible intervals (ribbon). The vertical line indicates the collection start date of age-specific death counts. (Middle) Estimated number of infectious individuals by age (posterior median). (Right) Estimated age-specific effective reproduction number, posterior median estimate (line) and 95% credible intervals (ribbon).

Downloaded from https://www.science.org on March 22, 2024



Downloaded from https://www.science.org on March 22, 2024

**Fig. 3. Time evolution of estimated age-specific SARS-CoV-2 reproduction numbers across the US.** Each panel shows, for the corresponding location (state or metropolitan area), the estimated posterior probability that the daily effective reproduction number from individuals stratified in seven age groups was below one. Darker colors indicate a low probability that reproduction numbers were below one.

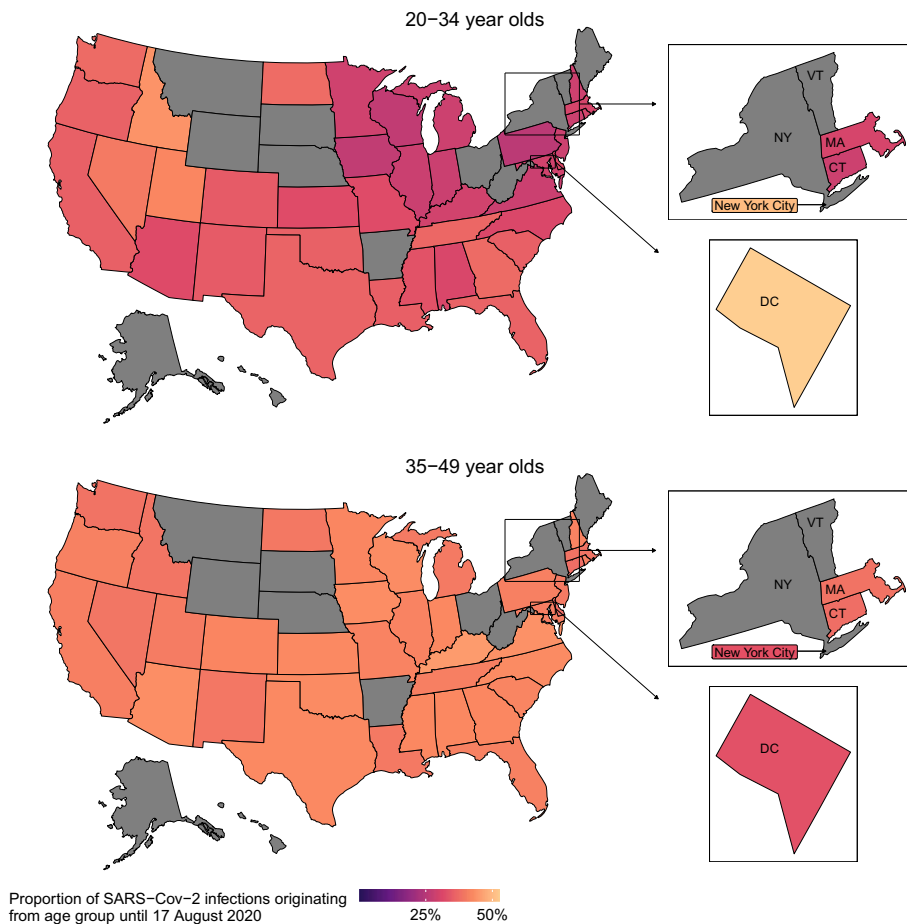


**Fig. 4. Estimated spatial variation in the share of young adults aged 20 to 34 and adults aged 35 to 49 to COVID-19 spread until mid-August 2020.** Posterior median estimates of the contribution to cumulated SARS-CoV-2 infections until 17 August 2020, prior to school reopening. State-level COVID-19 epidemics not considered in this study are in gray.

and provided 2570 observation days to estimate the impact of school reopening on COVID-19 spread. The following analyses are therefore based on fewer data points than those mentioned previously and rely on mortality figures accrued until the end of October 2020, as well as reported school case data from Florida and Texas, which were used to define lower and upper bounds on cumulative attack rates among children and teens aged 5 to 18 (see materials and methods). Reflecting stuttering transmission chains in school settings, reproduction numbers from children aged 0 to 9 and teens aged 10 to 19 were estimated at below one [respectively, 0.52 (0.42 to 0.60) and 0.73 (0.57 to 0.88)] after schools were considered to have reopened in the model (Fig. 3 and table S2). Reproduction numbers from children were lower than those from teens because at a population level, preschoolers have fewer contacts than school-aged children (fig. S6).

Since school closure mandates were lifted, the higher reproduction numbers from chil-

dren and teens resulted in age shifts in the sources of SARS-CoV-2 infections. In October 2020, an estimated 2.7% (1.8 to 3.7%) of infections originated from children aged 0 to 9, 7.1% (4.5 to 10.3%) from teens aged 10 to 19, 34.0% (31.9 to 36.4%) from adults aged 20 to 34, 38.2% (36.7 to 39.4%) from adults aged 35 to 49, 15.1% (14.1 to 16.1%) from adults aged 50 to 64, 2.5% (2.2 to 2.9%) from individuals aged 65 to 79, and 0.3% (0.2 to 0.3%) from individuals aged 80+ across all locations evaluated (compare table S5 and table S4). The reconstructed shifts in the age of COVID-19 sources after school reopening are relatively modest compared to the typical age profile of infection sources of pandemic influenza (21) and reflect a lower age-specific susceptibility to SARS-CoV-2 transmission among children and teens but also substantially fewer, inferred disease-relevant contacts from children and teens than would be expected from their corresponding prepandemic contact intensities. The mechanisms behind these beneficial effects remain unclear, but the model suggests

that they are substantial. In retrospective counterfactual scenarios, we explored what COVID-19 case and death trajectories would have been expected if schools had remained closed and find a large overlap between the counterfactual and actual case and death trajectories (Fig. 6 and fig. S15). However, because children and teens seed infections in older age groups that are more transmission efficient, as of October 2020, school opening is associated with an estimated 25.7% (14.5 to 40.5%) increase in COVID-19 infections and a 5.9% (3.4 to 9.3%) increase in COVID-19-attributable deaths (table S7). Larger proportions of COVID-19 infections and deaths are attributed to school reopening if the actual number of cases among school-aged children is more than six times as large as the number in school situation reports (table S7). These findings indicate that adults aged 20 to 34 and 35 to 49 continue to be the only age groups that contribute disproportionately to COVID-19 spread relative to their size in the population (fig. S14) and that the impact of school reopening on resurgent COVID-19 is mitigated most effectively by strengthening disease control among adults aged 20 to 49.

#### Caveats

The findings of this study need to be considered in the context of the following limitations. Rossen and colleagues (22) observed that US excess deaths between the beginning of the pandemic and October 2020 were 38% higher than the reported COVID-19-attributable deaths, suggesting that the death data on which this analysis rests are subject to underreporting. The scale of the US epidemics may be larger than we infer, and our age-specific analyses may be biased if underreporting of deaths depends on age. However, owing to the high proportion of asymptomatic COVID-19 cases (5), underreporting is a substantially larger caveat for reported case data, and in particular the observed shifts in the share of age groups among reported cases (4, 23), which are absent from the share of age groups among reported deaths (fig. S11). This suggests that age-specific death data provide a more reliable picture into resurgent COVID-19 epidemics than reported cases. We further rely on limited data from two contact surveys performed in the United Kingdom and China to characterize contact patterns from and to younger individuals during school-closure periods (7, 8), and this could have biased our findings that children and teens have contributed negligibly to SARS-CoV-2 spread until school reopening. To address this limitation, we explored the impact of higher intergenerational contact intensities involving children during school closure periods, and in these analyses the estimated contribution of children aged 0 to 9 onward spread until August 2020 remained

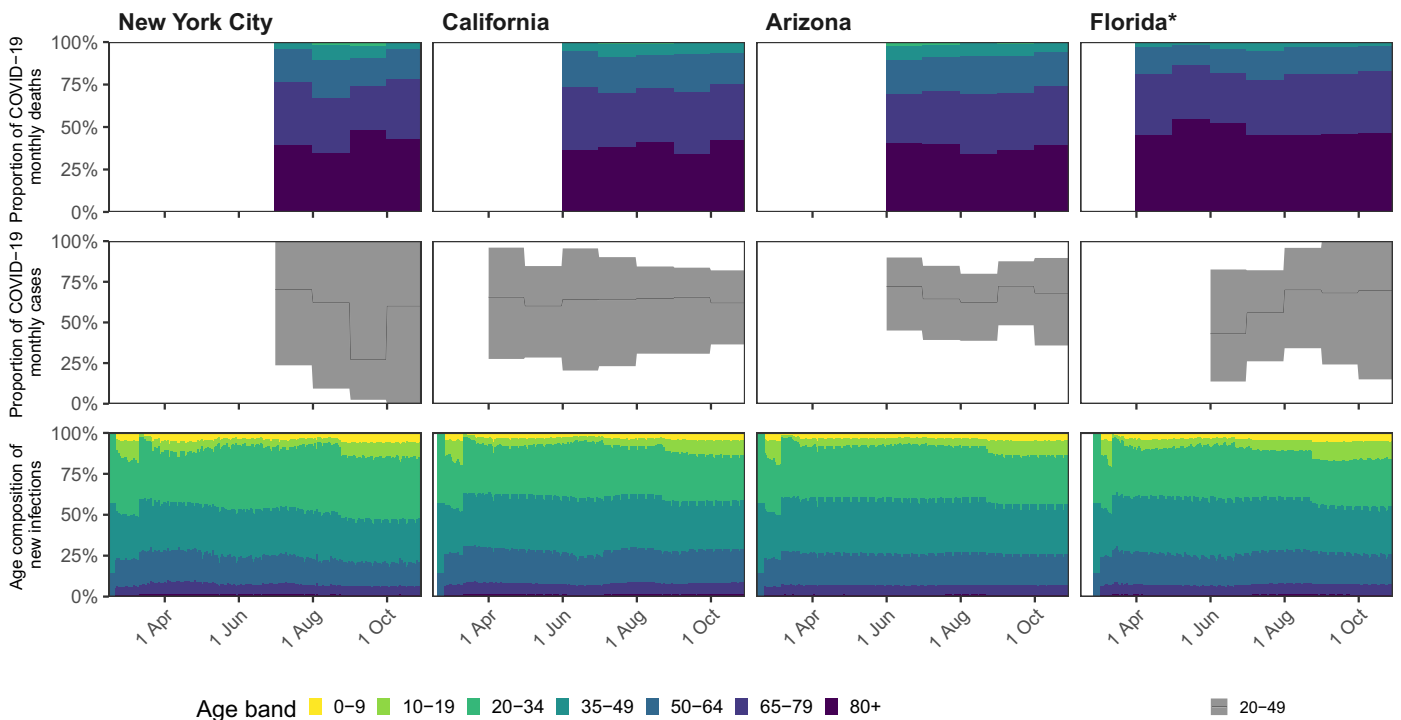


**Fig. 5. Share of age groups among COVID-19-attributable deaths and infections in the United States. (Top)** Proportion of monthly observed deaths attributed to COVID-19 by age group. Age-specific COVID-19-attributable deaths were recorded from state or city Departments of Health. Departments of Health used their own age stratification, and the observed data were re-estimated into common age groups across states with a Dirichlet-Multinomial model (see supplementary materials). An asterisk (\*) next to a location's name indicates that there was a statistically significant

shift in the share of individuals aged 80+ among deaths in the corresponding location. **(Middle)** Proportion of monthly reported cases among 20- to 49-year olds. Monthly cases were back-calculated using the meta-analysis infection fatality rate estimates of (20). The figure shows the estimated share of individuals aged 20 to 49 among monthly cases (posterior median: line, 95% credible interval: ribbon). **(Bottom)** New daily estimated infections by age group in New York City, Florida, California, and Arizona (posterior median).

below 5% and the contribution of teens aged 10 to 19 remained below 12.5% (see supplementary materials). Epidemiologic models are sensitive to assumptions about the infection fatality ratio (IFR) that enables the estimation of actual cases from observed deaths by age. Our analyses are based on a meta-analysis that consolidates estimates from 27 studies and 34 geographic locations (20). To test the assumed IFR, we compared the scale of the estimated resurgent epidemics against data from seroprevalence surveys conducted by the Centers for Disease Control and Prevention (CDC) (24) and found good congruence (table S6 and supplementary materials). The COVID-19 epidemic is more granular than considered in our spatial modeling approach. Substantial heterogeneity in disease transmission exists at the county level (25), and our situation analyses by state and metropolitan areas should be interpreted as averages. Without exception, the model underlying our analyses also relies on simplifying mathematical assumptions on population-level disease spread, which may be shown unsuitable as further evidence on SARS-CoV-2 transmission accumulates (26). For instance, the model assumes that children and teens transmit SARS-CoV-2 as readily as

do adults, which has been challenging to quantify to date (27), and falls short of accounting for population structure other than age, such as household settings, where attack rates have been estimated to be substantially higher than in non-household settings (28). It is possible that the model underestimates the impact of school reopening on SARS-CoV-2 transmission.

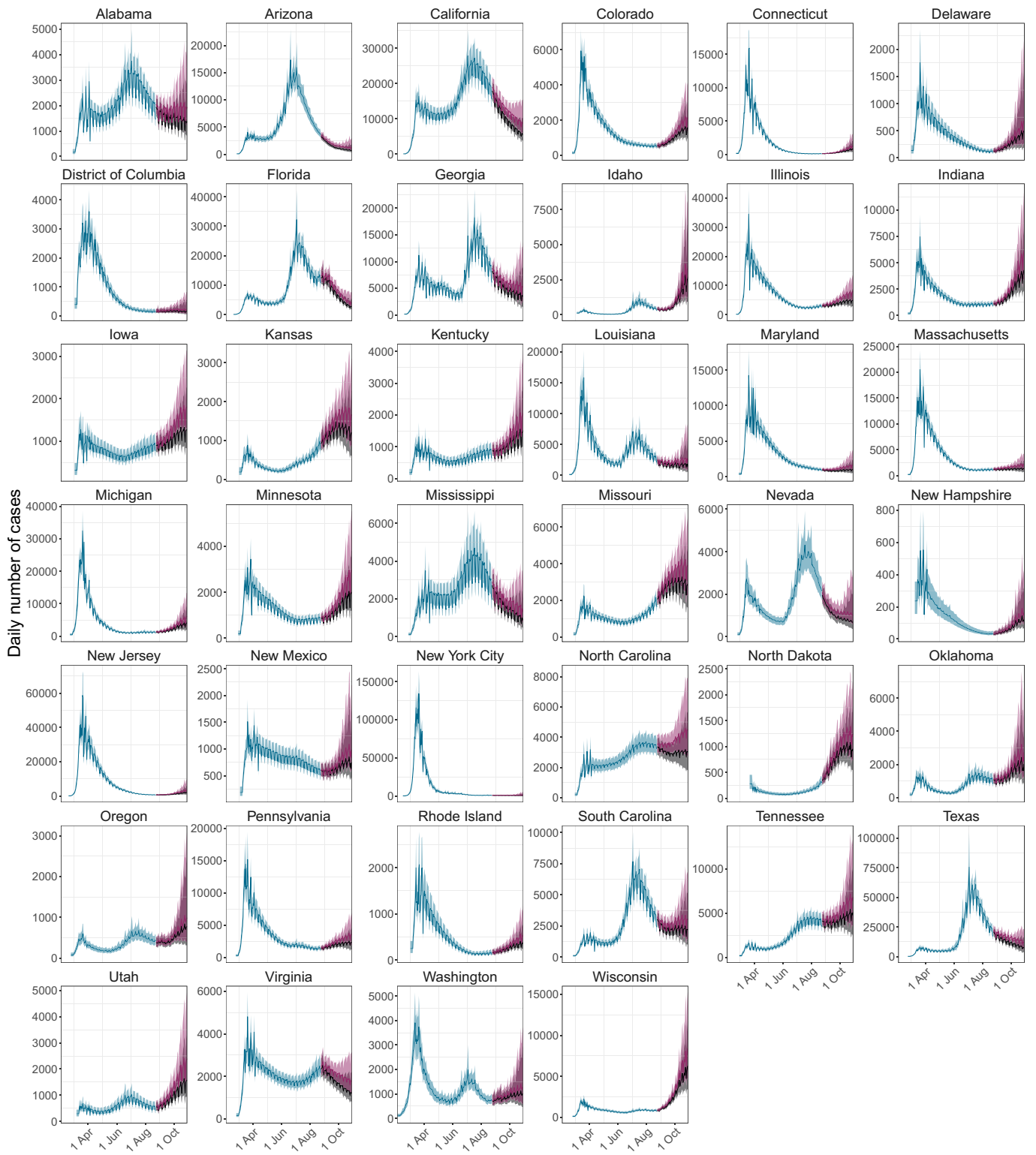
Data from countries that have reopened schools have provided little evidence for substantial transmission in schools, nor for significantly increased community-level infection rates after school reopening until the emergence of more transmissible SARS-CoV-2 variants (29, 30), but this might reflect frequent sub-clinical infection among school-aged children. More-transmissible SARS-CoV-2 variants could increase reproduction numbers to above one from all age groups, which implies substantial spread from all age groups, and require generally stricter control measures across all ages to prevent COVID-19-attributable deaths (31).

### Conclusions

This study provides evidence that the resurgent COVID-19 epidemics in the US in 2020 have been driven by adults aged 20 to 49 and, in

particular, adults aged 35 to 49, before and after school reopening. Unlike pandemic influenza, these adults accounted, after school reopening in October 2020, for an estimated 72.2% (68.6 to 75.9%) of SARS-CoV-2 infections in the US locations considered, whereas less than 5% originated from children aged 0 to 9 and less than 10% from teens aged 10 to 19. The population mobility data, and the death data provided by state and city Departments of Health, reveal heterogeneous disease spread in the US, with higher transmission risk per venue visit attributed to individuals aged 20 to 49 over distinct time periods and younger epidemics with a greater share of individuals aged 20 to 34 among cumulative infections in the southern, southwestern, and western regions of the US. Over time, the share of age groups among reported deaths has been markedly constant, suggesting that young adults are unlikely to have been the primary source of resurgent epidemics since summer 2020 and that, instead, changes in mobility and behavior among the broader group of adults aged 20 to 49 underlie resurgent COVID-19 in the US in 2020. This study indicates that in locations where novel, highly transmissible SARS-CoV-2 lineages have not yet become





■ Counterfactual scenario if kindergartens and elementary, middle, and high schools would have remained closed  
 ■ Fit to observed data, with kindergartens and elementary, middle and high schools re-opening unless statewide closure mandated

**Fig. 6. Retrospective counterfactual modeling scenarios exploring the impact of school reopening on COVID-19-attributable cases.** Shown in blue and red are estimated, daily COVID-19 cases (purple line, posterior median estimate; purple ribbon, 95% credible intervals) until 29 October 2020. The model was fitted to data including reported cases among school aged children in this period, assuming that reported cases could be an underestimate of actual cases among school aged children by a factor of 6 or less. In counterfactual modeling scenarios, the retrospective impact of continued school closures was explored until 29 October 2020, and the predicted case trajectories are shown (black line, posterior median estimate; black ribbon, 95% credible interval).

Downloaded from <https://www.science.org> on March 22, 2024

established, additional interventions among adults aged 20 to 49, such as mass vaccination with transmission-blocking vaccines, could bring resurgent COVID-19 epidemics under control and avert deaths.

### Materials and methods

To characterize the role of age groups in driving resurgent COVID-19, we have taken a systematic approach that involved data collection, mathematical modeling, likelihood-based inference, and validation against external data. The following sections summarize our materials and methods, and full technical details are in the Data Availability Statement and the supplementary Materials.

#### Data and data processing

The analyses presented in this study are based on age-specific COVID-19 attributable mortality counts that were collected daily from US state and city Departments of Health (DoH), all-age COVID-19 death counts, all-age COVID-19 case counts, COVID-19 case counts in school settings K1-K15, human contact data before and during the pandemic, and human mobility data during the pandemic.

Briefly, age-specific COVID-19 cumulative death counts were retrieved for 42 US states, the District of Columbia and New York City from city or state DoH websites, data repositories, or via data requests to DoH (table S8). Data were checked for consistency and adjusted when necessary. Age-specific COVID-19 death time series were reconstructed from cumulative counts, and the time series were used for model fitting (32).

All-age daily COVID-19 case and death counts from 1 February 2020 until 30 October 2020 regardless of age were obtained from Johns Hopkins University (JHU) for all US states and the District of Columbia (3), except New York City. For New York City, daily COVID-19 deaths counts were obtained from the GitHub Repository (33). The all-age death counts were used for model fitting prior to when age-specific death counts were reported for each location, and all-age case counts were used for model fitting for the entire study period.

COVID-19 case counts in school settings K1-K15 were retrieved for Florida and Texas and matched with student enrolment numbers in each school from the Common Core of Data Americas Public Schools database (34). Cumulative attack rates were obtained by dividing cumulative reported cases among students by student numbers, and used for model fitting.

Human contact data before the pandemic were obtained from the Polymod study (6), and used to predict baseline contact matrices during the early part of the pandemic for each location, similar as in (18). Given the variation

in contact patterns seen across survey settings, baseline contact matrices for each study location in the US were predicted based on each location's population density and age composition with a log linear regression model. Age-specific population counts were obtained from (35). Area measurements were obtained for every US state and for New York City, respectively, from (36) and (37). Contact matrices were predicted by 5-year age bands for weekdays and weekends, and used in the model. Human contact data during the pandemic were retrieved from two surveys (7, 8), and used in the model to specify contact patterns from and to individuals aged 0 to 19 during periods of school closure.

Age-specific human mobility trends were derived from the Foursquare Labs Inc. US first-party panel that includes >10 million of opt-in, always-on active users. From operated and partner apps, Foursquare collects a variety of device signals against opted-in users including intermittent device GPS coordinate pings, WiFi signals, cell signal strength, device model, and operating system version. A smaller set of labeled explicit check-ins is captured from a portion of the user panel. Check-ins are explicit confirmations that a user was at a given venue at a given point of time, and serve as training labels for a nonlinear model that is used to predict visits among users with unlabeled visits in terms of probabilities as to which venue users ultimately visited (17). Visit probabilities among panellists were processed and aggregated by day, age, and study location, and standardized to daily per capita visits using latest US Census data. Percent changes in daily venue visits by age and study location were obtained relative to the baseline period 3 February to 9 February 2020 and used for analysis and model fitting. For validation purposes, a second mobility data set was obtained from Emodo. The Emodo data set quantifies the proportion of individuals with at least one observed ping outside the user's home location, out of a panel of individuals whose GPS enabled devices emitted at least one ping on the corresponding day. Primary data were similarly aggregated by day, age, and study location, standardized to daily per capita visits using latest US Census data, and mobility trends were calculated relative to the baseline period 19 February to 3 March 2020.

#### Statistical analysis of human mobility data and COVID-19-attributable death data

The age-specific human mobility data showed marked time trends, which were characterized in terms of three phases defined by the dip date after which the 15-day moving average fell below 10% compared to the average value in the two prior weeks, and the rebound date that corresponded to the date at which the 15-day moving average was lowest. Differ-

ences in the mobility trends relative to the February baseline period, before and after rebound dates, and relative to individuals aged 35 to 44 were assessed using Gamma regression models using log link and location by age interaction covariates.

To characterize the time evolution of deaths across locations and validate model fits, age-specific COVID-19-attributable deaths among the same age strata across locations were predicted by month with a Dirichlet-Multinomial regression model. Trends in the share of age groups among monthly deaths were assessed by testing for differences in the proportions in the first month relative to subsequent months.

To test for potential differences in age-specific transmission dynamics based on the collected death data and without epidemic models, meta-analysis estimates of age-specific infection fatality ratios (20) were used to predict the share of age groups among infections from monthly age-specific deaths. Trends in the share of age groups among monthly infections were assessed by testing for differences in the proportions in the first month relative to subsequent months.

#### Contact-and-infection model

To quantify age-specific aspects of COVID-19 spread in heterogeneous populations, we formulated an age-specific, discrete-time renewal model in which disease transmission occurs via contact intensities between population groups stratified by 5-year age bands. The model has four key features described below. First, contact intensities vary in time and are inferred from signatures in the age-specific mortality and mobility data. This feature aims to reflect the substantial changes in human contact patterns during the pandemic (7-9). Second, the challenge and value of the model to produce generalizable knowledge is to explain disease spread across multiple locations with distinct demographics simultaneously. To this end, the renewal equations were embedded into a hierarchical model in which information on disease spread is borrowed across locations (1, 38). Third, the model describes disease spread during the initial and later phase of the pandemic, as mobility patterns become less correlated with transmission risk and schools reopen (39, 40). This feature allowed us to test for changes in disease dynamics over time. Fourth, the model is fitted in a Bayesian framework to the all-age and age-specific death data, all-age case data, case data from schools, and age-specific human mobility trends (41). This feature forced us to focus on a model whose parameters are inferable from the data across all locations. The model is described in detail in the supplementary materials.

Briefly, we consider populations stratified by the 5-year age bands  $A$ , such that

$$a \in A = \{[0-4], [5-9], \dots, [75-79], [80-84], [85+]\} \tag{1}$$

and denote the number of new infections,  $c$ , on day  $t$ , in age group  $a$ , and location  $m$  as  $c_{m,t,a}$ . In the renewal equation, past infections are weighted by their relative infectiousness on day  $t$ , and the sum of these individuals has contacts with individuals in other age groups. Contacts are described by the expected number of disease relevant human contacts one person in age group  $a$  has with other individuals in age group  $a'$  on day  $t$  in location  $m$ ,  $c_{m,t,a,a'}$ . Upon contact, a proportion  $s_{m,t,a}$  of individuals in age group  $a'$  on day  $t$  in location  $m$  remains susceptible to SARS-CoV-2 infection, and transmission occurs with probability  $\rho_{a'}$ . Thus, the age-specific renewal equation with time-changing contact intensities is

$$c_{m,t,a'} = s_{m,t,a'} \rho_{a'} \sum_a c_{m,t,a,a'} \left( \sum_{s=1}^{t-1} c_{m,s,a} g(t-s) \right) \tag{2}$$

where  $g$  quantifies the relative infectiousness of individuals  $s$  days after infection. An important feature of SARS-CoV-2 transmission is that similarly to other coronaviruses but unlike pandemic influenza (42), susceptibility to SARS-CoV-2 infection increases with age (7, 21, 43). Here, we used contact tracing data from Hunan province, China (7) to specify lower susceptibility to SARS-CoV-2 infection among children aged 0 to 9, and higher susceptibility among individuals aged 60+, when compared to the 10 to 59 age group as part of the transmission probabilities  $\rho_{a'}$ . Previously infected individuals are assumed to be immune to re-infection within the analysis period, consistent with mounting evidence for sustained antibody responses to SARS-CoV-2 antigens (44, 45), so that

$$s_{m,t,a'} = 1 - \frac{\sum_{s=1}^{t-1} c_{m,s,a'}}{N_{m,a'}}, \tag{3}$$

where  $N_{m,a'}$  denotes the population count in age group  $a'$  and location  $m$ .

For adults aged 20+, the time changing contact intensities were described in terms of the prepandemic baseline contact intensities in location  $m$ , which we denote by  $C_{m,t,a,a'}$ , and expected reductions in disease relevant contacts from contacting individuals of age  $a$  on day  $t$  in location  $m$ , which we denote by  $\eta_{m,t,a}$ , and contacted individuals of age  $a'$  on day  $t$  in location  $m$ ,  $\eta_{m,t,a'}$

$$C_{m,t,a,a'} = \eta_{m,t,a} C_{m,a,a'} \eta_{m,t,a'}, \tag{4}$$

where  $a, a' \in \{[20-24], \dots, [85+]\}$ . Expected reductions in disease relevant contacts were

specified as a random effects model that included the observed age-specific mobility trends as covariates. In the model, each age-specific mobility trend was decoupled into three separate covariates that reflect the initial pre-pandemic, dip, and rebound phases in human mobility trends, so that previously observed decreases in correlation between mobility trends and transmission risk could be captured (40, 41, 46). As the same number of venue visits in, e.g., Wyoming may translate to different transmission risk than in e.g., New York City, spatial random effects allowed for scaling of mobility trends during the dip and rebound phase in each location. As venue visits do not capture all aspects of transmission risk, the model further incorporates independently for each location autocorrelated biweekly random effects to capture information on elevated, disease relevant contact intensities and transmission risk that is present in the death time series data. To test for age-specific signatures of elevated transmission risk, the model further included for each location age-specific random effects for individuals aged 20 to 49.

For children and teens aged 0 to 20, mobility data are not available, and during periods of school closure the contact intensities from and to children and teens were set to the average contact intensities reported in (7). This implied that relative to pre-pandemic contact patterns, peer-based contacts were substantially reduced, whereas contacts from an adult to children and teens increased slightly. In the model, schools were set to reopen on or after 24 August 2020 when state administrations no longer mandated statewide school closures by that date (47, 48). Thereafter, Eq. 4 was extended to include children and teens, and expected mobility reductions were estimated from the case and death data. In the absence of further data, a common average effect could be estimated across locations and children and teen age groups for the last two observation months,  $\eta_{m,t,a} = \eta^{\text{children}}$  for  $a \in [0-20]$ . A further compound effect  $\gamma$  was added to modulate the number of disease relevant child/teen child/teen contacts, which we interpreted as reduced infectiousness from children and teens and/or a positive impact of non-pharmaceutical interventions among school aged children and teens.

### Bayesian inference

Past age-specific disease dynamics across all locations were inferred from age-specific death data available across locations, and age-specific mobility data. To do this, in the model, a proportion  $\pi_{m,a}$  of new infections in location  $m$  of age  $a$  die, and the day of death is determined by the infection-to-death distribution, which was assumed to be constant across age groups. The proportions  $\pi_{m,a}$  were associated with a strongly informative prior

derived from the meta-analysis of (20), but were allowed to deviate from the baseline infection fatality ratio through location-specific random effects. The expected number of deaths in location  $m$  on day  $t$  in age group  $a$ ,  $d_{m,t,a}$ , were aggregated to the reporting strata in each location, and fitted to the observed data using a Negative Binomial likelihood model. When age-specific death data were not available, the model was fitted to all-age death data with a Negative Binomial likelihood model. All-age case data were smoothed, and used to specify a lower bound on the overall number of infections  $c_{m,t} = \sum_a c_{m,t,a}$  through a student-t cumulative density likelihood model. Case data from schools were used to calculate empirical attack rates in school settings during specified observation windows. In turn, the empirical attack rates were used to describe a lower bound on the actual attack rate among 5 to 18-year-old children and teens in the same observation periods in the model, using a normal cumulative density likelihood model. An upper bound on the actual attack rates was also specified by assuming that actual cases in school settings were underreported at most 10-fold, using a normal complementary cumulative density likelihood model. The contact-and-infection model was fitted with CmdStan release 2.23.0 (22 April 2020), using an adaptive Hamiltonian Monte Carlo (HMC) sampler (41). 8 HMC chains were run in parallel for 1,000 iterations, of which the first 400 iterations were specified as warm-up. There were no divergent transitions.

### Generated quantities

Results were reported in the age bands  $d \in D = \{[0-9], [10-19], [20-34], [35-49], [50 \text{ to } 64], [65 \text{ to } 79], [80+]\}$ . The primary model outputs were aggregated correspondingly, e.g. the number of new infections in location  $m$  on day  $t$  in reporting age group  $d$  was  $c_{m,t,d} = \sum_{a \in d} c_{m,t,a}$ . The effective number of infectious individuals  $c^*$  in location  $m$  and age group  $d$  on day  $t$  was calculated based on the renewal model (2),  $c_{m,t,d}^* = \sum_{s=1}^{t-1} c_{m,s,d} g(t-s)$ , and is shown in Fig. 2.

Following (2), the time-varying reproduction number on day  $t$  from one infectious person in age group  $a$  in location  $m$  is  $R_{m,t,a} = \sum_a s_{m,t,a'} \rho_{a'} C_{m,t,a,a'}$ , and the reproduction numbers were aggregated to the reporting strata based on the identity  $R_{m,t,d} = \sum_{a \in d} (c_{m,t,a}^* / (\sum_{k \in d} c_{m,t,k}^*) R_{m,t,a})$ , and are shown in Fig. 2 and tables S1 and S2. The transmission flows from age group  $a$  to age group  $a'$  at time  $t$  in location  $m$  are given by  $F_{m,t,a,a'} = s_{m,t,a'} \rho_{a'} C_{m,t,a,a'} \left( \sum_{s=1}^{t-1} c_{m,s,a} g(t-s) \right)$ , and are aggregated using  $F_{m,t,d,d'} = \sum_{a \in d, a' \in d'} F_{m,t,a,a'}$ . In

turn, the contributions of age groups to COVID-19 spread are  $S_{m,t,d} = (\sum_d F_{m,t,d,d}) / (\sum_d \sum_d F_{m,t,d,d})$ , and are reported in tables S4. Cumulated COVID-19 attack rates were calculated through  $A_{m,t,d} = (\sum_{s=1}^t c_{m,s,d}) / (N_{m,d})$ , where  $N_{m,d}$  is the number of individuals in location  $m$  and age group  $d$ , and are reported in table S6.

#### Validation and sensitivity analyses

Reconstructed past transmission dynamics were assessed against external data on the scale of the epidemic from seroprevalence surveys conducted across the US by the CDC (24). Validation results are reported in the supplementary materials, suggesting larger discrepancies between model fit and seroprevalence data for Connecticut and New York City, with larger epidemics reconstructed in the model than the data suggest. The contact-and-infection model does not account for sustained spatial importation of SARS-CoV-2 infections such as from New York City to Connecticut, and may have over-estimated the magnitude of self-sustaining epidemic in locations receiving sustained SARS-CoV-2 importations. However, we also note that the Connecticut seroprevalence estimates predict an infection to observed case ratio that is substantially below those of the other CDC seroprevalence studies. The inferred contact patterns were assessed against external data from the BICS study that quantified human contact patterns during the pandemic (9). Validation results are reported in the supplementary materials, suggesting similarly strong reductions in human contact intensities as in the survey data. Disaggregated by age, the model reproduces highest contact intensities among 35- to 44-year-old individuals, comparatively lower contact intensities from individuals aged 45+, and largest reductions in contact intensities from individuals aged 25 to 34. The survey data suggest that contact intensities from individuals aged 18 to 24 could be higher than reconstructed through the contact-and-infection model, but we also note large confidence intervals around the survey estimates.

Sensitivity analyses were conducted to assess central modeling assumptions on the infection fatality ratio, contact intensities among children and teens during periods of school closure, relative susceptibility of children and teens to SARS-CoV-2 infection, and are reported in the supplementary materials. Our findings on the age groups that drive SARS-CoV-2 transmission were found to be robust to these assumptions.

#### REFERENCES AND NOTES

- S. Flaxman *et al.*, Estimating the effects of non-pharmaceutical interventions on COVID-19 in Europe. *Nature* **584**, 257–261 (2020). doi: [10.1038/s41586-020-2405-7](https://doi.org/10.1038/s41586-020-2405-7); pmid: [32512579](https://pubmed.ncbi.nlm.nih.gov/32512579/)
- S. Pei, S. Kandula, J. Shaman, Differential effects of intervention timing on COVID-19 spread in the United States. *Sci. Adv.* **6**, eabd6370 (2020). doi: [10.1126/sciadv.abd6370](https://doi.org/10.1126/sciadv.abd6370); pmid: [33158911](https://pubmed.ncbi.nlm.nih.gov/33158911/)
- E. Dong, H. Du, L. Gardner, An interactive web-based dashboard to track COVID-19 in real time. *Lancet Infect. Dis.* **20**, 533–534 (2020). doi: [10.1016/S1473-3099\(20\)30120-1](https://doi.org/10.1016/S1473-3099(20)30120-1); pmid: [32087114](https://pubmed.ncbi.nlm.nih.gov/32087114/)
- T. K. Boehmer *et al.*, Changing age distribution of the COVID-19 pandemic – United States, May–August 2020. *Morbidity and Mortality Weekly Report* **69**, 1404–1409 (2020). doi: [10.15585/mmwr.mm6939e1](https://doi.org/10.15585/mmwr.mm6939e1); pmid: [33001872](https://pubmed.ncbi.nlm.nih.gov/33001872/)
- E. Lavezzo *et al.*, Suppression of a SARS-CoV-2 outbreak in the Italian municipality of Vo'. *Nature* **584**, 425–429 (2020). doi: [10.1038/s41586-020-2488-1](https://doi.org/10.1038/s41586-020-2488-1); pmid: [32604404](https://pubmed.ncbi.nlm.nih.gov/32604404/)
- J. Mossong *et al.*, Social contacts and mixing patterns relevant to the spread of infectious diseases. *PLOS Med.* **5**, e74 (2008). doi: [10.1371/journal.pmed.0050074](https://doi.org/10.1371/journal.pmed.0050074); pmid: [18366252](https://pubmed.ncbi.nlm.nih.gov/18366252/)
- J. Zhang *et al.*, Changes in contact patterns shape the dynamics of the COVID-19 outbreak in China. *Science* **368**, 1481–1486 (2020). doi: [10.1126/science.abb8001](https://doi.org/10.1126/science.abb8001); pmid: [32350060](https://pubmed.ncbi.nlm.nih.gov/32350060/)
- C. I. Jarvis *et al.*, Quantifying the impact of physical distance measures on the transmission of COVID-19 in the UK. *BMC Med.* **18**, 124 (2020). doi: [10.1186/s12916-020-01597-8](https://doi.org/10.1186/s12916-020-01597-8); pmid: [32375776](https://pubmed.ncbi.nlm.nih.gov/32375776/)
- Feehan, D. M., Mahmud, A., Quantifying population contact patterns in the United States during the COVID-19 pandemic. *medRxiv* 2020.04.13.20064014 [Preprint]. 29 August 2020). doi: [10.1101/2020.04.13.20064014](https://doi.org/10.1101/2020.04.13.20064014)
- S. Chang *et al.*, Mobility network models of COVID-19 explain inequities and inform reopening. *Nature* **589**, 82–87 (2021). doi: [10.1038/s41586-020-2923-3](https://doi.org/10.1038/s41586-020-2923-3); pmid: [33171481](https://pubmed.ncbi.nlm.nih.gov/33171481/)
- A. Waksman, "Phones, Lambdas and the Joy of Snap-to-Place Technology" (2018); <https://enterprise.foursquare.com/intersections/article/phones-lambdas-and-the-joy-of-snap-to-place-tech/>.
- L. L. C. Google, "COVID-19 Community Mobility Reports" (2020); <https://www.google.com/covid19/mobility>
- YouGov PLC, "Personal measures taken to avoid COVID-19" (2020); <https://today.yougov.com/topics/international/articles-reports/2020/03/17/personal-measures-taken-avoid-covid-19>
- K. A. Fisher *et al.*, Community and Close Contact Exposures Associated with COVID-19 Among Symptomatic Adults ≥18 Years in 11 Outpatient Health Care Facilities - United States, July 2020. *MMWR Morb. Mortal. Wkly. Rep.* **69**, 1258–1264 (2020). doi: [10.15585/mmwr.mm6936a5](https://doi.org/10.15585/mmwr.mm6936a5); pmid: [32915165](https://pubmed.ncbi.nlm.nih.gov/32915165/)
- N. E. Williams, T. A. Thomas, M. Dunbar, N. Eagle, A. Dobra, Measures of Human Mobility Using Mobile Phone Records Enhanced with GIS Data. *PLOS ONE* **10**, e0133630 (2015). doi: [10.1371/journal.pone.0133630](https://doi.org/10.1371/journal.pone.0133630); pmid: [26192322](https://pubmed.ncbi.nlm.nih.gov/26192322/)
- D. K. Chu *et al.*, Physical distancing, face masks, and eye protection to prevent person-to-person transmission of SARS-CoV-2 and COVID-19: A systematic review and meta-analysis. *Lancet* **395**, 1973–1987 (2020). doi: [10.1016/S0140-6736\(20\)31142-9](https://doi.org/10.1016/S0140-6736(20)31142-9); pmid: [32497510](https://pubmed.ncbi.nlm.nih.gov/32497510/)
- K. E. C. Ainslie *et al.*, Evidence of initial success for China exiting COVID-19 social distancing policy after achieving containment. *Wellcome Open Res.* **5**, 81 (2020). doi: [10.12688/wellcomeopenres.15843.2](https://doi.org/10.12688/wellcomeopenres.15843.2); pmid: [32500100](https://pubmed.ncbi.nlm.nih.gov/32500100/)
- K. Prem *et al.*, Projecting contact matrices in 177 geographical regions: an update and comparison with empirical data for the COVID-19 era. *medRxiv* 2020.07.22.20159772 [Preprint]. 28 July 2020. <https://doi.org/10.1101/2020.07.22.20159772>
- H. Unwin *et al.*, Report 23 - State-level tracking of COVID-19 in the United States: A subnational analysis with future scenarios. *Imperial College London COVID-19 Reports* (2020); <https://doi.org/10.25561/79231>
- A. T. Levin *et al.*, Assessing the age specificity of infection fatality rates for COVID-19: Systematic review, meta-analysis, and public policy implications. *Eur. J. Epidemiol.* **35**, 1123–1138 (2020). doi: [10.1007/s10654-020-00698-1](https://doi.org/10.1007/s10654-020-00698-1); pmid: [33289900](https://pubmed.ncbi.nlm.nih.gov/33289900/)
- N. G. Davies *et al.*, Age-dependent effects in the transmission and control of COVID-19 epidemics. *Nat. Med.* **26**, 1205–1211 (2020). doi: [10.1038/s41591-020-0962-9](https://doi.org/10.1038/s41591-020-0962-9); pmid: [32546824](https://pubmed.ncbi.nlm.nih.gov/32546824/)
- L. M. Rossen, A. M. Branum, F. B. Ahmad, P. Sutton, R. N. Anderson, Excess Deaths Associated with COVID-19, by Age and Race and Ethnicity - United States, January 26–October 3, 2020. *Morbidity and Mortality Weekly Report* **69**, 1522–1527 (2020). doi: [10.15585/mmwr.mm6942e2](https://doi.org/10.15585/mmwr.mm6942e2); pmid: [33090978](https://pubmed.ncbi.nlm.nih.gov/33090978/)
- European Center for Disease Prevention and Control, "Coronavirus disease 2019 (COVID-19) in the EU/EEA and the UK eleventh update: resurgence of cases"; <https://www.ecdc.europa.eu/en/publications-data/rapid-risk-assessment-coronavirus-disease-2019-covid-19-eueea-and-uk-eleventh>
- F. P. Havers *et al.*, Seroprevalence of Antibodies to SARS-CoV-2 in 10 Sites in the United States, March 23–May 12, 2020. *JAMA Intern. Med.* **180**, 1576–1586 (2020). doi: [10.1001/jamainternmed.2020.4130](https://doi.org/10.1001/jamainternmed.2020.4130); pmid: [32692365](https://pubmed.ncbi.nlm.nih.gov/32692365/)
- W. Messner, S. E. Payson, Variation in COVID-19 outbreaks at the US state and county levels. *Public Health* **187**, 15–18 (2020). doi: [10.1016/j.puhe.2020.07.035](https://doi.org/10.1016/j.puhe.2020.07.035); pmid: [32889227](https://pubmed.ncbi.nlm.nih.gov/32889227/)
- I. Holmdahl, C. Buckee, Wrong but useful - what COVID-19 epidemiologic models can and cannot tell us. *N. Engl. J. Med.* **383**, 303–305 (2020). doi: [10.1056/NEJMp2016822](https://doi.org/10.1056/NEJMp2016822); pmid: [32412711](https://pubmed.ncbi.nlm.nih.gov/32412711/)
- R. M. Viner *et al.*, Susceptibility to SARS-CoV-2 infection among children and adolescents compared with adults: A systematic review and meta-analysis. *JAMA Pediatr.* (2020). doi: [10.1001/jamapediatrics.2020.4573](https://doi.org/10.1001/jamapediatrics.2020.4573); pmid: [32975552](https://pubmed.ncbi.nlm.nih.gov/32975552/)
- Q.-L. Jing *et al.*, Household secondary attack rate of COVID-19 and associated determinants in Guangzhou, China: A retrospective cohort study. *Lancet Infect. Dis.* **20**, 1141–1150 (2020). doi: [10.1016/S1473-3099\(20\)30471-0](https://doi.org/10.1016/S1473-3099(20)30471-0); pmid: [32562601](https://pubmed.ncbi.nlm.nih.gov/32562601/)
- European Center of Disease Prevention and Control, "COVID-19 in children and the role of school settings in COVID-19 transmission - first update" (2020); <https://www.ecdc.europa.eu/en/publications-data/children-and-school-settings-covid-19-transmission>
- G. Vogel, "School risk calculations scrambled by fast-spreading virus strains" (2020); <https://www.sciencemag.org/news/2021/01/new-coronavirus-variant-scrambles-school-risk-calculations>
- E. Volz *et al.*, Transmission of SARS-CoV-2 Lineage B.1.1.7 in England: Insights from linking epidemiological and genetic data. *medRxiv* 2020.12.30.20249034 [Preprint]. 4 January 2021. <https://doi.org/10.1101/2020.12.30.20249034>
- Imperial College London COVID-19 Response Team, "COVID-19 Age specific Mortality Data Repository" (2020); <https://github.com/ImperialCollegeLondon/US-covid19-agespecific-mortality-data>
- New York City Department of Health, "Coronavirus data" (2020); <https://github.com/nychealth/coronavirus-data/blob/master/totals/by-age.csv>
- National Centre for Education Statistics, "Common Core of Data America's School database" (2020); <https://nces.ed.gov/ccd/>
- United States Census Bureau, "Age and Sex American Community Survey by U.S. States, 2018 Census" (2018); <https://www.census.gov/data.html>
- United States Census Bureau, "State Area Measurements and Internal Point Coordinates" (2010); <https://www.census.gov/geographies/reference-files/2010/geo/state-area.html>
- Wikipedia, "New York City" (2019); [https://en.wikipedia.org/wiki/New\\_York\\_City](https://en.wikipedia.org/wiki/New_York_City)
- A. Gelman *et al.*, *Bayesian Data Analysis* (CRC Press, 2013).
- IHME COVID-19 Forecasting Team, Modeling COVID-19 scenarios for the United States. *Nat. Med.* **27**, 94–105 (2021). pmid: [33097835](https://pubmed.ncbi.nlm.nih.gov/33097835/)
- P. Nouvellet *et al.*, Report 26 - Reduction in mobility and COVID-19 transmission. *Imperial College London COVID-19 Reports* (2020); <https://doi.org/10.25561/79643>
- B. Carpenter *et al.*, Stan: A Probabilistic Programming Language. *J. Stat. Softw.* **76**, 1–32 (2017). doi: [10.18637/jss.v076.i01](https://doi.org/10.18637/jss.v076.i01)
- R. M. Anderson *et al.*, Epidemiology, transmission dynamics and control of SARS: The 2002–2003 epidemic. *Philos. Trans. R. Soc. Lond. B Biol. Sci.* **359**, 1091–1105 (2004). doi: [10.1098/rstb.2004.1490](https://doi.org/10.1098/rstb.2004.1490); pmid: [15306395](https://pubmed.ncbi.nlm.nih.gov/15306395/)
- E. Goldstein, M. Lipsitch, M. Cevik, On the effect of age on the transmission of SARS-CoV-2 in households, schools and the community. *J. Infect. Dis.* **2020**. doi: [10.1093/infdis/jiaa691](https://doi.org/10.1093/infdis/jiaa691); pmid: [33119738](https://pubmed.ncbi.nlm.nih.gov/33119738/)
- A. S. Iyer *et al.*, Dynamics and significance of the antibody response to SARS-CoV-2 infection. *medRxiv* 10.1101/2020.07.18.20155374 [Preprint]. 20 July 2020. <https://doi.org/10.1101/2020.07.18.20155374>
- I. Schullien *et al.*, Characterization of pre-existing and induced SARS-CoV-2-specific CD8<sup>+</sup> T cells. *Nat. Med.* **27**, 78–85 (2021). doi: [10.1038/s41591-020-10143-2](https://doi.org/10.1038/s41591-020-10143-2); pmid: [33184509](https://pubmed.ncbi.nlm.nih.gov/33184509/)

46. A. C. Miller *et al.*, Mobility trends provide a leading indicator of changes in SARS-CoV-2 transmission. *medRxiv* 10.1101/2020.05.07.20094441 [Preprint]. 11 May 2020. <https://doi.org/10.1101/2020.05.07.20094441>.
47. T. Hale *et al.*, Variation in US states responses to COVID-19. *Blavatnik School of Government* (2020); [www.bsg.ox.ac.uk/covidtracker](http://www.bsg.ox.ac.uk/covidtracker).
48. Education Week, "Map: Coronavirus and School Closures" (2020); <https://www.edweek.org/ew/section/multimedia/map-coronavirus-and-school-closures.html>.
49. M. Monod, A. Blenkinsop, X. Xi, H. J. Unwin, M. Swapnil, O. Ratmann, ImperialCollegeLondon/covid19model: Age groups that sustain resurging COVID-19 epidemics in the United States, Version 11.0, Zenodo (2021); <https://doi.org/10.5281/ZENODO.4461896>.

#### ACKNOWLEDGMENTS

We thank the Imperial College COVID-19 Response Team for their insightful comments: K. E. C. Ainslie, A. Boonyasiri, O. Boyd, L. Cattarino, L. V. Cooper, Z. Cucunubá, G. Cuomo-Dannenburg, B. Djaafara, I. Dorigatti, R. FitzJohn, K. A. M. Gaythorpe, L. Geidelberg, W. D. Green, A. Hamlet, W. Hinsley, B. Jeffrey, E. Knock, D. Laydon, G. Nedjati-Gilani, P. Nouvellet, K. V. Parag, I. Siveroni, H. A. Thompson, R. Verity, C. E. Walters, H. Wang, Y. Wang, O. J. Watson, P. Winskill, C. Whittaker, P. G. T. Walker, C. A. Donnelly, L. Okell, B. Sangeeta, N. F. Brazeau, O. D. Eales, D. Haw, N. Imai, E. Jauneikaite, J. Lees, A. Mousa, D. Olivera, J. Skaup, and L. Whittles. **Funding:** This work was supported by the NIHR HPRU in Modelling and Health Economics, a partnership between PHE, Imperial College London and LSHTM (grant code NIHR200908), and the

Imperial College Research Computing Service. We acknowledge funding from the Imperial College COVID-19 Response Fund; the Bill & Melinda Gates Foundation; the EPSRC, through the EPSRC Centre for Doctoral Training in Modern Statistics and Statistical Machine Learning at Imperial and Oxford; and the MRC Centre for Global Infectious Disease Analysis (reference MR/R015600/1), jointly funded by the UK Medical Research Council (MRC) and the UK Foreign, Commonwealth, and Development Office (FCDO), under the MRC-FCDO Concordat agreement and that is also part of the EDCTP2 program supported by the European Union. We thank Microsoft and Amazon for providing cloud computing services. The views expressed are those of the authors and not necessarily those of the United Kingdom (UK) Department of Health and Social Care, the National Health Service, the National Institute for Health Research (NIHR), or Public Health England (PHE) **Author contributions:** O.R. conceived the study. A.G., S.M., S.F., S.B., N.F., and O.R. oversaw the study. M.M., D.H., S.Be., S.T., Y.C., M.McM., M.H., H.Z., A.Be., and O.R. oversaw and performed data collection. M.M., A.Bl., X.X., and O.R. led the analysis. V.C.B., H.C., S.F., J.I.H., T.M., A.G., H.J.T.U., M.V., S.W., and S.M. contributed to the analysis. All authors discussed the results and contributed to the revision of the final manuscript. **Competing interests:** S.B. acknowledges the National Institute for Health Research (NIHR) BRC Imperial College NHS Trust Infection and COVID themes, the Academy of Medical Sciences Springboard award and the Bill and Melinda Gates Foundation. OR reports grants from the Bill & Melinda Gates Foundation during the conduct of the study. **Data and materials availability:** The Foursquare population mobility data are available on Github, <https://github.com/ImperialCollegeLondon/covid19model>, under the Creative

Commons Attribution-NonCommercial-NoDerivs 4.0 International Public License. The Emodo population mobility data are available on Github, <https://github.com/ImperialCollegeLondon/covid19model>, and Zenodo (49) (for updates see (32)), under the Creative Commons Attribution-NonCommercial 4.0 International Public License. Code are available on Github, <https://github.com/ImperialCollegeLondon/covid19model>, under the MIT License. This work is licensed under a Creative Commons Attribution 4.0 International (CC BY 4.0) license, which permits unrestricted use, distribution, and reproduction in any medium, provided the original work is properly cited. To view a copy of this license, visit <https://creativecommons.org/licenses/by/4.0/>. This license does not apply to figures/photos/artwork or other content included in the article that is credited to a third party; obtain authorization from the rights holder before using such material.

#### SUPPLEMENTARY MATERIALS

[science.sciencemag.org/content/371/6536/eabe8372/suppl/DC1](https://science.sciencemag.org/content/371/6536/eabe8372/suppl/DC1)  
Supplementary Text  
Figs. S1 to S15  
Tables S1 to S7  
References (50–118)  
State-Level Situation Reports  
MDAR Reproducibility Checklist  
18 September 2020; accepted 27 January 2021  
Published online 2 February 2021  
10.1126/science.abe8372